

Topology-Aware Integrated Communication, Sensing, and Power Transfer for SAGIN

Han Yu^{*}, Jiajun He[†], Xinpeng Yi[‡], Feng Yin[§], Hing Cheung So[¶], and Giuseppe Caire^{*}

^{*} Faculty of Electrical Engineering and Computer Science, Technical University of Berlin, Germany

[†] Centre for Wireless Innovation (CWI), Queen's University Belfast, BT3 9DT Belfast, U.K.

[‡] National Mobile Communications Research Laboratory, Southeast University, Nanjing 210096, China

[§] School of Artificial Intelligence, The Chinese University of Hong Kong, Shenzhen, China

[¶] Department of Electrical Engineering, City University of Hong Kong, Hong Kong SAR, China

Abstract—The space-air-ground integrated network (SAGIN) has garnered significant attention in recent years due to its capability to extend communication networks from terrestrial environments to near-ground and space contexts. The application of SAGIN enables to achieve a high-quality, multi-functional, and complex communication requirements, which are essential for sixth-generation communication systems. This paper presents a topology aware (TA) framework to leverage the topological structure in SAGIN to address the multi-functional communication challenge, particularly the integrated sensing, communication, and power transfer (ISCPT) problem. To take advantage of the topological structure, we initially establish the topology according to the criteria of visibility and channel strength. The ISCPT problem can be reformulated into a topological structure as a mixed integer linear program, providing valuable insights from the objectives and constraints. Results demonstrate the superior performance of our solution compared to the benchmarks.

Index Terms—Integrated sensing, communication, and wireless power transfer, multi-user, topology satellite network.

I. Introduction

In recent years, space-air-ground integrated networks (SAGINs) have garnered considerable attention as a promising paradigm for achieving global, robust, and high-quality communication services [1]. Various companies and institutions start working on SAGIN e.g., OneWeb, SpaceX, and it has been widely used in many areas including earth observation, mapping, disaster rescue [2]. With the advancement of non-terrestrial communication technologies, SAGINs are expected to provide not only reliable communication but also additional functionalities such as sensing, localization, and wireless power transfer (WPT) [3]. In the context of SAGINs, research on multi-functional problem, e.g., integrated sensing and communication (ISAC) has been extensively explored. For example, Yin et al. [4] have investigated ISAC in low-Earth orbit (LEO) satellite networks and proposed a rate-splitting multiple access (RSMA) scheme to balance sensing and communication performance. In addition, deep learning has been adopted for joint optimization of the transmit waveform and receive filter [5].

The topology-aware (TA) approach has been successfully applied in terrestrial networks, demonstrating significant performance gains [6]. Notably, SAGINs inherently

possess well-defined and sparse topological structures. This is because a) multiple satellites act as distributed access points (APs), b) both inter-satellite and satellite-to-ground links primarily consider free-space path loss [7], and c) each user is typically connected to only a limited number of satellites. These characteristics collectively result in a much sparser topology compared to terrestrial communication networks. Motivated by these reasons, this paper proposes a TA solution for the multi-functional integrated sensing, communication, and power transfer (ISCPT) problem, aiming to achieve balanced performance across sensing, communication, and charging. This work focuses on the static topological structure, while dynamic extensions will be investigated in future research.

To our knowledge, this is the first work to leverage the network topological structure to address multi-functional optimization in SAGINs. The contributions of this paper are threefold. First, we introduce two topology-based criteria, namely, visibility and channel strength, to represent user-satellite connectivity and interference relationships. The multiple objectives corresponding to the key functionalities of the SAGIN, i.e., communication, sensing, and WPT, are expressed into the topological structure. The TA ISCPT problem is then formulated as a mixed-integer linear program (MILP). Simulation results show that the proposed TA-based scheme achieves superior communication and sensing performance while maintaining acceptable power transfer efficiency.

II. System Model

As illustrated in Fig. 1, we consider a multi-user SAGIN comprising M LEO satellites that function as APs, along with multiple satellite users supporting communication, sensing, and WPT functionalities. Terrestrial users also request communication services from the satellites. A central unit (CU) satellite is considered to facilitate optimization and decision-making processes. The CU is only required to know the topological structure, meaning there is only occasional information exchange between the CU and APs. For clarity, we define the following user sets: $\mathcal{K}_C \triangleq \mathcal{K}_{C,T} \cup \mathcal{K}_{C,S}$, where \mathcal{K}_C denotes the set of all communication users, $\mathcal{K}_{C,T}$ and $\mathcal{K}_{C,S}$ are the set

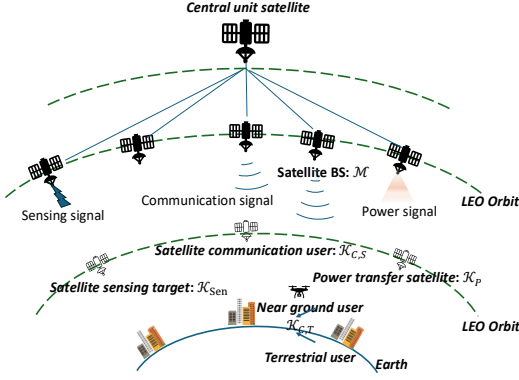


Fig. 1: SAGIN comprises APs and multiple terrestrial and satellite users. This network consists of the LEO constellation in higher orbits, which includes multiple satellite APs. A subset of LEO satellites acts as satellite users, facilitating communication, sensing, and wireless power transfer. In addition, the network incorporates terrestrial users for communication purposes.

of terrestrial and satellite communication users, satellite communication users, respectively. Furthermore, the other satellite users can be subdivided into two categories: 1) \mathcal{K}_P , the set of satellite users requiring charging via WPT, and 2) \mathcal{K}_{Sen} , where $|\mathcal{K}_{\text{Sen}}| = 1$, the set of satellite sensing targets. We define the set $\mathcal{K} \triangleq \mathcal{K}_C \cup \mathcal{K}_P \cup \mathcal{K}_{\text{Sen}}$ to denote all users. In addition, our system defines the term ‘terrestrial user’ to encompass both terrestrial and near-ground users.

A. Coordinate Transformation

Before establishing the objectives for communication, sensing, and WPT, we first introduce the coordinate transformation for satellite APs and terrestrial users. To compute the distance between satellite APs and terrestrial users, we adopt the Earth-centered, Earth-fixed (ECEF) coordinate system [7]. The transformation from latitude, longitude, and altitude (LLA) coordinates to ECEF coordinates follows the model in [8] is:

$$\mathbf{l} = \begin{bmatrix} x \\ y \\ z \end{bmatrix} = \begin{bmatrix} (N+H) \cos B \cos L \\ (N+H) \cos B \sin L \\ [N(1-e^2) + H] \sin B \end{bmatrix}, \quad (1)$$

where (B, L, H) represents the latitude, longitude, and height, respectively; $e = \frac{\sqrt{\alpha^2 - \beta^2}}{\alpha}$ denotes the first eccentricity, while α, β are the semi-major and semi-minor axes of the ellipsoid; N denotes the prime vertical radius of curvature, i.e.: $N = \frac{\alpha}{\sqrt{1 - e^2 \sin^2 B}}$. Since the connectivity between satellite APs and terrestrial users depends not only on distance but also on the elevation angle, a user can be served by a satellite only if the elevation angle exceeds a predefined threshold. Otherwise, the connection is considered infeasible. For evaluating the elevation between the satellite AP and the terrestrial users, it is necessary to convert the ECEF coordinates (x, y, z) of the satellites into east-north-up (ENU) coordinates [9] based on the LLA position of the terrestrial user, i.e., $\text{EAST} = -\Delta x \sin L + \Delta y \cos L$,

$\text{NORTH} = -\Delta x \sin B \cos L - \Delta y \sin B \sin L + \Delta z \cos B$, $\text{UP} = \Delta x \cos B \cos L + \Delta y \cos B \sin L + \Delta z \sin B$, where $\Delta x, \Delta y$, and Δz represent the positional differences in ECEF coordinates between the satellite and the terrestrial user.

B. Communication Model

To achieve the objectives of ISOPT in multi-user SAGIN, the transmit signal from the m -th AP is given by: $s_m = \sum_{k \in \mathcal{K}_C} s_{mk} x_k + s_{ms}$, where $\sum_{k \in \mathcal{K}_C} |s_{mk}|^2 + |s_{ms}|^2 = 1$ is the precoder for communication and sensing functionalities, x_k denotes the transmitted symbol for k -th user. The signal received by the k -th communication user is:

$$y_k = \underbrace{\sum_{m=1}^M \sqrt{\rho_m} h_{mk} s_{mk} x_k}_{\text{Desired signal}} + \underbrace{\sum_{m=1}^M \sqrt{\rho_m} h_{mk} s_{ms}}_{\text{Interference from sensing signal}} + \underbrace{\sum_{m=1}^M \sum_{k' \neq k, k' \in \mathcal{K}_C} \sqrt{\rho_m} h_{mk} s_{mk'} x_{k'}}_{\text{Interference from communication users}} + \underbrace{n_k}_{\text{Noise}}, \quad (2)$$

where h_{mk} is the channel between the m -th AP and the k -th user, ρ_m is the power for each AP, $n \sim \mathcal{N}_{\mathbb{C}}(0, \sigma^2)$ denotes the additive white Gaussian noise (AWGN), G_B and G_U denote the antenna gains from the AP and user sides, respectively. The channel h_{mk} can be written as $h_{mk} = w_{mk} \sqrt{G_B G_U} e^{-\frac{2\pi}{\lambda} d_{mk}}$, where w_{mk}^2 denotes the path loss, and $\lambda = \frac{c}{f}$ is the wave length, c is the light speed, and f denotes the carrier frequency. Due to differences in size and hardware characteristics between terrestrial and satellite equipment, distinct antenna gains are employed. The specific parameters are provided in Section V. In the context of the non-terrestrial system, we define the path loss by focusing solely on the line-of-sight (LoS) channel: $w_{mk}^2 = 20 \log \left(\frac{4\pi d_{mk}}{\lambda} \right)$, $\phi_e \geq \tau_\phi$, $k \in \mathcal{K}$, where d_{mk} is the distance between the m -th AP satellite and the k -th user. By leveraging the coordinate transformation from the LLA to ECEF based on (1), we can write $d_{mk} = \|\mathbf{l}_m - \mathbf{l}_k\|_2$. Therefore, the sum rate is adopted as one of the objectives in the ISOPT system to evaluate communication performance, which is given by $R_c = \sum_{k \in \mathcal{K}} \log(1 + \gamma_k)$, where γ_k is the signal-to-interference-plus-noise ratio (SINR) of the k -th user:

$$\gamma_k = \frac{|\sum_{m=1}^M \sqrt{\rho_m} h_{mk} s_{mk}|^2}{\sum_{k' \in \mathcal{K}_C} |\text{IC}_{k'}|^2 + |\text{IS}|^2 + \sigma^2}, \quad k \in \mathcal{K}_C \quad (3)$$

where IC and IS denote the interference from communication and sensing, respectively. They are written as:

$$\text{IC}_{k'} = \sum_{m=1}^M \sqrt{\rho_m} h_{mk} s_{mk'}, \quad \text{IS} = \sum_{m=1}^M \sqrt{\rho_m} h_{mk} s_{ms}. \quad (4)$$

C. Sensing Model and Wireless Power Transfer

The satellite yielding the highest sensing SINR is selected for the positioning, navigation, and timing (PNT) purposes. Note that PNT using a single satellite AP is commonly considered, since multiple time-of-arrival (ToA) measurements are feasible because the satellite moves

dynamically along its orbit, providing varying observation points for ToA collection [10]. Since the measurement error depends on the sensing SINR, we analyze the sensing SINR as follows. During the sensing procedure, each AP employs a distinct precoder, which leads to interference and degrades the localization performance. Consequently, the signal received at the sensing target is:

$$y_s = \underbrace{\sqrt{\rho_{m_s}} h_{m_s s} s_{m_s s}}_{\text{Desired sensing signal}} + \underbrace{\sum_{k \in \mathcal{K}_C} \sum_{m=1}^M \sqrt{\rho_m} h_{m s} s_{m k} x_k}_{\text{Interference from communication users}} + \underbrace{n}_{\text{Noise}}, \quad (5)$$

where m_s is the selected AP for sensing. Regarding the sensing objective, we adopt the sensing SINR as the evaluation performance matrix, which can be written as [11]

$$\gamma_s = \frac{\rho_{m_s} |h_{m_s s} s_{m_s s}|^2}{\sum_{k \in \mathcal{K}_C} \left| \sum_{m=1}^M \sqrt{\rho_m} h_{m s} s_{m k} \right|^2 + \sigma^2}. \quad (6)$$

This work focuses on satisfying the sensing SINR requirement rather than implementing a specific localization algorithm. The details on satellite-based target localization can be found in [10]. Based on the communication and sensing models in (3) and (6), the power received by the charging users is: $E_p =$

$$\sum_{k_p \in \mathcal{K}_P} \left(\underbrace{\sum_{k \in \mathcal{K}_C} \left| \sum_{m=1}^M \rho_m h_{m k_p} s_{m k} \right|^2}_{\text{Power from communication users}} + \underbrace{\left| \sum_{m=1}^M \rho_m h_{m k_p} s_{m s} \right|^2}_{\text{Power from sensing user}} \right).$$

III. Topological Structure Model

A. Bipartite Graph Construction

Based on the topology of SAGINs, we define the bipartite graph as $\mathcal{G} = (\mathcal{M}, \mathcal{K}, \mathcal{E})$, where \mathcal{M} denotes the set of APs, \mathcal{K} denotes the set of all users, and $\mathcal{E} = e(m, k)$ denotes the edges. To determine the sparse connectivity of the joint network, we evaluate link availability from two key aspects: 1) visibility and 2) channel strength [12]. When a connection is unavailable due to the lack of visibility, the corresponding channel is treated as nonexistent in both the topological graph and the actual system, effectively represented as a “zero link”. In contrast, connections that are visible but exhibit weak channel strength are excluded from the topological graph. However, they may still exist in the physical system and potentially cause interference to other users. The following section provides a detailed definition of how connectivity is determined.

- **Visibility of Satellite-Terrestrial Users:** The visibility between a satellite and a terrestrial user is determined by the elevation angle, which can be computed through the transformation of ENU coordinates, i.e.: $\phi_{mk} = \arctan \left(\frac{\text{UP}}{\sqrt{\text{NORTH}^2 + \text{EAST}^2}} \right)$. For the terres-

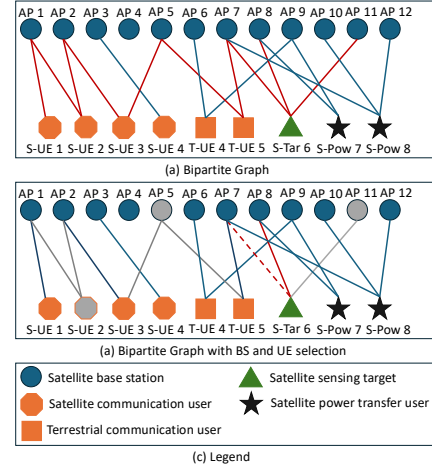


Fig. 2: (a) shows the bipartite graph with the connection between APs and users. (b) shows the result involving the AP and user selection. The solid lines represent the strong link utilized for precoder generation, while the dashed line indicates the strong link not employed for this purpose, although interference must be taken into account. Gray nodes indicate that the nodes are closed, while gray lines represent the disappeared strong links resulting from closing the nodes.

trial user:

$$e(m, k) = \begin{cases} 1, & \phi_{mk} \geq \tau_\phi, m \in \mathcal{M}, k \in \mathcal{K}_{C,T} \\ 0, & \phi_{mk} < \tau_\phi, m \in \mathcal{M}, k \in \mathcal{K}_{C,T} \end{cases} \quad (7)$$

- **Visibility of Satellite-Satellite Users:** The visibility condition of the inter-satellite link (ISL) is determined by the minimum distance from the line connecting two satellites to Earth, which is: $d_{mk,e}^{\min} = \frac{\sqrt{\|\mathbf{l}_m\|_2^2 \|\mathbf{l}_k\|_2^2 - (\mathbf{l}_m^T \mathbf{l}_k)^2}}{\|\mathbf{l}_m - \mathbf{l}_k\|_2}$. Intuitively, if the shortest distance from the line connecting two satellites to the Earth’s center is less than the Earth’s radius, the direct LOS between them is obstructed by the Earth; otherwise, the satellites are mutually visible. Based on this criterion, the ISL visibility condition is:

$$e(m, k) = \begin{cases} 1, & d_{mk,e}^{\min} \geq R_{\text{Earth}}, m \in \mathcal{M}, k \in \mathcal{K}_S \\ 0, & d_{mk,e}^{\min} < R_{\text{Earth}}, m \in \mathcal{M}, k \in \mathcal{K}_S \end{cases} \quad (8)$$

where we define the satellite user set as $\mathcal{K}_S \triangleq \mathcal{K}_{C,S} \cup \mathcal{K}_P \cup \mathcal{K}_{\text{Sen}}$, and $K_S = |\mathcal{K}_S|$.

- **Channel Strength:** This condition is used to determine the weak link by comparing the pathloss with the defined threshold. Thus, to the ISL edge, we have

$$e(m, k) = \begin{cases} 1, & w_{mk} \geq \tau_{\text{PL}}, m \in \mathcal{B}, k \in \mathcal{K}_S \\ 0, & w_{mk} < \tau_{\text{PL}}, m \in \mathcal{B}, k \in \mathcal{K}_S \end{cases} \quad (9)$$

Consequently, a bipartite graph can be constructed, as illustrated in Fig. 2(a). We see that different shapes are used to represent APs and users. Blue edges indicate valid communication links, while red edges represent interference that must be considered. All edges are determined based on the defined visibility and channel strength criteria. Each user is connected to only a limited subset of APs, and some APs have no connectivity to any users due to visibility constraints or weak channel

conditions. In addition, it is observed that conflict links between charging users and other users do not constitute interference links. This is because no specific precoding is applied to the charging users over these links.

B. Objective Reformulation based on Topological Structure

Fig. 2(a) indicates notable interference within the system, which degrades overall performance—particularly in communication and sensing functionalities. It is evident that selectively deactivating certain APs or users can significantly reduce interference. We see that communication satellite users, S-UEs 1, 2, 3, and 5, experience link conflicts at the AP side, resulting in performance degradation. In addition, sensing target, S-Tar 6, is impacted by interference from communication users due to overlapping connections on specific APs. As discussed in Section II, each sensing target selects a single AP for signal reception, while signals from other APs—regardless of whether they transmit the sensing precoder—are treated as interference. Accordingly, the three strongest links associated with S-Tar 6 are depicted as red solid lines to highlight potential interference sources. To mitigate this interference, selected users and APs can be deactivated. As shown in Fig. 2(b), disabling satellite user and APs: S-UE 2, AP 5, and AP 11, significantly reduces interference. Most of the red interference links are eliminated through this selective deactivation strategy. Note that the deactivation of S-UE 2 only indicates that it is not scheduled for service in the current timeslot. In subsequent timeslots, this user may be selected for service, while those served in the current timeslot may be temporarily deactivated. Such a dynamic scheduling mechanism can ensure long-term fairness and guarantee that all users are eventually served. In this paper, however, we focus exclusively on the optimization problem within a single timeslot, while fairness problem across multiple timeslots will be investigated in our future work. For the sensing target, S-Tar 6, AP 8 has been chosen as the sensing AP, while AP 7 is activated solely to serve the terrestrial user, T-UE 5. In this instance, S-Tar 6 continues to experience interference from the communication precoder transmitted by AP 7 to T-UE 5. This interference is not mitigated by deactivating either AP 7 or T-UE 5. There are two reasons for this. Firstly, the edge $e(m_7, k_6)$ does not affect T-UE 5. Moreover, maintaining this AP and user has no significant impact on the sensing SINR, keeping it above the defined threshold. Thus, based on the above discussion, we are able to design the precoder by controlling: 1) the user status; 2) the AP status; 3) the selected AP for the sensing target.

The objectives can be re-expressed based on the topological structure and the corresponding bipartite graph. Before presenting the formulation, we first introduce fundamental concepts related to bipartite graphs. The adjacency matrix of the bipartite graph \mathcal{G} is defined as \mathbf{A} . If a connection exists, i.e., $e(m, k) = 1$, then we have

$[\mathbf{A}]_{m,k} = 1$. In \mathbf{A} , the first K_C columns correspond to the communication connections; the $K_C + 1$ -th column denotes the sensing target connections; and the last K_P columns represent the connections of charging users. Since we focus on the dominant connections as stated in Section II, we define the weight matrix \mathbf{W} to denote the dominant path loss, and each element of \mathbf{W} is defined as $\hat{w}_{mk} = w_{mk}[\mathbf{A}]_{m,k}$. In this paper, maximum ratio transmission (MRT) is employed solely for the purpose of expressing key objectives, namely communication rate, sensing SINR, and received energy, in order to provide analytical clarity and actionable insights for algorithm and strategy design. The proposed algorithm and framework can also be extended to other precoding schemes, such as zero-forcing and minimum mean squared error, allowing performance to be assessed from various perspectives. By ignoring transmit power normalization, the objectives can be approximated under the topological structure based on AP and user selection as:

$$R_{c,T} = \sum_{k \in \mathcal{K}_C} u_k R_{k,T} = \sum_{k \in \mathcal{K}_C} u_k \log(1 + \gamma_{k,T}) \quad (10)$$

$$\gamma_{k,T} = \frac{\sum_{m=1}^M v_m \hat{w}_{mk}^2}{\sum_{m=1}^M (\sum_{k' \neq k} u_{k'} v_m \hat{w}_{mk'} \hat{w}_{mk} + v_m^s \hat{w}_{mk} \hat{w}_{ms}) + \sigma^2}, \quad (11)$$

$$\gamma_{s,T} = \frac{\sum_{m=1}^M v_m^s \hat{w}_{ms}^2}{\sum_{k \in \mathcal{K}_C} u_k \sum_{m=1}^M v_m \hat{w}_{mk} \hat{w}_{ms} + \sigma^2}, \quad (12)$$

$$E_{p,T} = \sum_{k_p \in \mathcal{K}_P} \sum_{m=1}^M \left(\sum_{k \in \mathcal{K}_C} u_k v_m \hat{w}_{mk_p} \hat{w}_{mk} + v_m^s \hat{w}_{mk_p} \hat{w}_{ms} \right), \quad (13)$$

where $R_{c,T}$, $\gamma_{k,T}$, $\gamma_{s,T}$, and $E_{p,T}$ denote the topology-based sum rate, communication and sensing SINR, and the total energy received for the charging users. Binary parameters $u_k, v_m, v_m^s \in \{0, 1\}$ are utilized to control the user, AP status, and the selection of the sensing AP. Regarding u_k and v_m , the value of ‘0’ indicates a deactivated status, while ‘1’ denotes an activated status. v_m^s represents the selection of the m -th AP for sensing. Given that only one AP is selected for the sensing target, we define $\sum_{m=1}^M v_m^s = 1, v_m^s \leq v_m$.

IV. Optimization Problem

As previously stated, the multi-user SAGIN aims to meet the requirements of communication, sensing, and power transfer, which is a multi-objective optimization problem as

$$\max R_c \quad \min \gamma_s \quad \max E_p. \quad (14)$$

$$\text{s.t. } \rho_m \leq \rho_{\max} \quad (15)$$

Notably, the power constraint can be eliminated in this topology-based optimization, as the power allocation is absorbed within the TA precoder design. The satellite power constraints are implicitly imposed with overall power limits, and the actual power is evenly allocated

according to the specified topology. In Section V, the power can be allocated equally, referred to as average power allocation, or proportionally, known as proportional power allocation.

This optimization involves three objectives: the first objective refers to the communication metric, specifically the sum rate of all activated communication users; the second relates to the quality of the sensing target; and the third evaluates the received energy for power transfer users. The communication is defined as the main task; thus, we represent the multi-objective optimization into a single objective optimization, considering the power transfer and sensing SINR as the constraints:

$$(\mathcal{P}) \quad \max \sum_{k \in \mathcal{K}_C} u_k R_{k,T} \quad (16a)$$

$$\text{s.t. } \gamma_s \geq \tau_s, \quad (16b)$$

$$E_{p,T} \geq \tau_p, \quad (16c)$$

where we use τ_s and τ_p to denote the performance thresholds of sensing and power, respectively.

Regarding the communication performance, as proven in [13], the multiplexing gain of the sum rate can be converted in terms of the maximum cardinality matching problem within the bipartite graph, taking into account the AP and the user-selected subgraph. The subgraph is defined as $\mathcal{G}' = (\mathcal{B}', \mathcal{K}'_C, \mathcal{E}')$, where \mathcal{B}' and \mathcal{K}'_C represent the selected communication node sets, and \mathcal{E}' comprises the edges associated with these selected nodes. Furthermore, as discussed in [6], the communication SINR for each selected user must also be considered as a constraint. Consequently, \mathcal{P} is approximately written as:

$$(\mathcal{P}') \quad \max |\mathcal{M}(\mathcal{B}', \mathcal{K}'_C)| \quad (17a)$$

$$\text{s.t. } \gamma_{k,T} \geq \tau_c, \quad \forall k \in \mathcal{K}'_C \quad (17b)$$

$$\gamma_{s,T} \geq \tau_s, \quad (17c)$$

$$E_{p,T} \geq \tau_p, \quad (17d)$$

where $|\mathcal{M}(\mathcal{B}', \mathcal{K}'_C)|$ denotes the maximum cardinality bipartite matching number of the selected subgraph. This subgraph includes communication user nodes alone, as only these users have the binary selection.

The optimization problem (\mathcal{P}'_c) can be approximated as a MILP, denoted by (\mathcal{P}''), which can be efficiently solved using MATLAB solvers. The obtained solution is feasible for the original problem (\mathcal{P}'_c). The MILP is:

$$(\mathcal{P}'') \quad \max_{u_k, v_m, v_m^s, z_{m,k}} \sum_{m=1}^M \sum_{k \in \mathcal{K}_C} z_{m,k} \quad (18a)$$

$$\text{s.t. } u_k \leq \sum_{m=1}^M [\mathbf{A}]_{m,k} v_m, \quad \forall k \in \mathcal{K}_C, \quad (18b)$$

$$v_m \leq \sum_{k \in \mathcal{K}_C} [\mathbf{A}]_{m,k} u_k + [\mathbf{A}']_{m,1} + \sum_{k_p \in \mathcal{K}_P} [\mathbf{A}']_{m,k_p}, \quad \forall m \in \mathcal{M} \quad (18c)$$

$$z_{m,k} \leq [\mathbf{A}]_{m,k}, \quad \forall k \in \mathcal{K}_C, m \in \mathcal{M} \quad (18d)$$

$$\sum_{k \in \mathcal{K}_C} z_{m,k} \leq v_m, \quad \forall m \in \mathcal{M} \quad (18e)$$

$$\sum_{m=1}^M z_{m,k} \leq u_k, \quad \forall k \in \mathcal{K}_C \quad (18f)$$

$$\hat{w}_{mk}^2 + c_1(1 - u_k) + c_2(1 - v_m) \geq \left(\sum_{k' \in \mathcal{K}_C} u_{k'} \hat{w}_{mk'} \hat{w}_{mk} + v_m^s \hat{w}_{ms} \hat{w}_{mk} \right) \hat{\tau}_{c,m}, \quad \forall k \in \mathcal{K}_C, m \in \mathcal{M} \quad (18g)$$

$$\sum_{k_p \in \mathcal{K}_P} \sum_{m=1}^M v_m \hat{w}_{mk_p} \geq \hat{\tau}_p \sum_{k_p \in \mathcal{K}_P} \sum_{m=1}^M \hat{w}_{mk_p}, \quad (18h)$$

$$\sum_{m=1}^M v_m^s \hat{w}_{ms}^2 + c_4(1 - u_k) \geq \hat{\tau}_{s,k} \left(\sum_{m=1}^M v_m^s \hat{w}_{ms}^2 + \sum_{m=1}^M v_m \hat{w}_{mk} \hat{w}_{ms} \right), \quad \forall k \in \mathcal{K}_C \quad (18i)$$

$$v_m^s \leq v_m, \quad \forall m \in \mathcal{M} \quad (18j)$$

$$\sum_{m=1}^M [\mathbf{A}]_{m,1} v_m^s = 1, \quad (18k)$$

$$u_k, v_m, v_m^s \in \{0, 1\}, \quad \forall k \in \mathcal{K}_C, m \in \mathcal{M} \quad (18l)$$

$$z_{m,k} \in [0, 1], \quad \forall k \in \mathcal{K}_C, m \in \mathcal{M} \quad (18m)$$

where $\hat{\tau}_{c,m}, \hat{\tau}_p, \hat{\tau}_{s,k} \in [0, 1]$ are thresholds for controlling the communication SINR, power transfer, sensing SINR, respectively. Here, c_1, c_2, c_3 , and c_4 are sufficiently large constants, and $z_{m,k}$ can be relaxed from binary value, i.e., $z_{m,k} = \{0, 1\}$ to $[0, 1]$ [13].

Remark 1. To the communication objective, the sum-rate, can be decomposed into two parts: the maximum matching problem, which determines the prelog factor, and the SINR constraint, ensuring the required communication quality of service (QoS). Specifically, the objective function (18a) characterizes the maximum matching cardinality. Constraint (18b) specifies that each activated communication user must be associated with at least one AP, while constraint (18c) requires that each activated AP serves either one activated communication user, one sensing target, or one power transfer user. The matching relationships are further governed by constraints (18d)–(18f). The communication SINR requirement is captured by constraint (18g). The charging limitations from the constraint (16c) are enforced through constraint (18h). Finally, constraints (18i)–(18k) are derived from the sensing requirement (16b).

The topological structure-based expression provides insights regarding each objective through the constraints. Constraint (18g) indicates that for each dominant connection of every user, the desired power must exceed the total received power by a specified percentage, $\hat{\tau}_{c,m}$. If not, the relevant AP or user should be deactivated. Additionally, this constraint illustrates the relationship of communication interference based on specific decisions regarding the

user and AP status. In this context, we utilize sufficiently large constants c_1 and c_2 to demonstrate the conditions under which both the user and the AP are activated, requiring the evaluation of the constraint. For instance, when $u_k = 1$ and $v_m = 0$, indicating that the user is activated while the AP is deactivated, the constraint must be satisfied. Conversely, when $u_k = 1$ and $v_m = 1$, it is necessary to determine whether the interference meets with the specified percentage, $\hat{\tau}_{c,m}$. Different with the communication and sensing functions, the charging power primarily relies on the status of the AP. Therefore, (18h) represents the received power by all charging users in relation to the corresponding AP status. The threshold $\hat{\tau}_p \in [0, 1]$ indicates the minimum amount of power that can be transferred from APs. Specifically, ‘0’ indicates that the charging function is entirely unnecessary, while ‘1’ means that all dominant connections of the charging user are required. The sensing SINR constraint (18i) is employed to select the sensing AP by comparing the interference connections for each communication user. The constraint (18k) states the requirement of selecting one existing dominant connection to the sensing target.

V. Numerical Results

A. Simulation Setups

TABLE I: Simulation Parameters.

Parameter	Value	Parameter	Value
G_B	30 dBi	G_U (Satellite)	30 dBi
G_U (Terrestrial)	40 dBi	f	2 GHz
W	100 MHz	ρ_{\max}	10 dB
$\hat{\tau}_p$	0.5	$\hat{\tau}_{s,k}$	0.5
K_P	4	$\hat{\tau}_{c,m}$	0.5
τ_ϕ	15°	τ_{PL}	-190 dB

This section evaluates the performance of the proposed optimization and greedy algorithms in terms of communication, sensing, and WPT. We consider a system where LEO satellites serve as both APs and users, with the user satellites positioned in lower orbits relative to the LEO APs. Two distinct LEO constellations are constructed to represent the satellite APs and users. The AP constellation operates at an altitude of 700 km and consists of 16 orbital planes, while the user constellation is deployed at an altitude of 300 km with 4 orbital planes. Both constellations comprise 128 satellites each, and we randomly select 30 LEOs from the user constellation as the LEO users. We also consider the terrestrial users located around at 5 remark cities: Berlin (52.52°, 13.4°); New York (40.71°, -74°); London (50.5°, -0.13°); Beijing (39.9°, 116.4°); and Sydney (-33.87°, 151.21°). The system parameters are provided in the Table I.

B. Results

The performance of the TA-ISCPPT algorithm is evaluated by comparing with the greedy user selection, and a baseline with no selection. We present the performance of the proposed approach in terms of sum rate, sensing SINR, and received power as functions of the number of APs M , as shown in Figs 3. Firstly, Fig.

3(a) indicates that the proposed TA-ISCPPT optimization demonstrates superior communication performance. Secondly, while the orthogonality-based greedy user selection mitigates interference among users, the performance does not exhibit a significant improvement compared to ‘No selection.’ The ‘Greedy user selection’ method results in a limited number of activated users, leading to a low prelog factor. In our proposed TA optimization method, deactivating certain appropriate APs and allowing partial non-orthogonality among users may result in significant performance improvements. Fig. 3(b) is the received power performance across different approaches. The ‘No selection’ and ‘Greedy user selection’ exhibit the same received power, as both methods do not deactivate the APs. The distinction between the benchmark and the proposed TA optimization lies in the power loss resulting from the deactivation of APs. Nevertheless, the power loss for the ‘TA Optimization’ is marginally over 5 dBm, which is deemed acceptable.

Fig. 3(c) plots the sensing SINR for three different approaches. The ‘Greedy user selection’ achieves optimal sensing SINR by mitigating interference from communication users and selecting the AP with the strongest channel. The TA-based method demonstrates acceptable performance, which is significantly better than ‘No selection’ but is inferior to the optimal benchmark, since we do not adopt a very large sensing threshold. Furthermore, it is evident that the ‘No selection’ and ‘TA optimization’ schemes demonstrate superior performance with a limited number of APs, as they exhibit a lower probability of overlap with communication users. However, the optimal performance of the ‘No selection’ method presents a contrasting situation compared to others. This is due to the fact that ‘No selection’ selects the strongest AP to the sensing target. As the number of APs increases, there is a higher probability of including an AP with greater channel strength compared to the scheme with a lower number of APs.

VI. Conclusion

This paper investigated the ISCPPT problem within a multi-user SAGIN framework. A TA framework was developed to establish connectivity between users and satellite APs based on two criteria: visibility and channel strength, facilitated the physical interpretation of communication, sensing, and WPT objectives. The ISCPPT problem was reformulated within a topological framework as a solvable MILP. The TA framework has been validated by addressing the ISCPPT problem and is anticipated to be a promising method for SAGINs.

References

- [1] J. Ye et al., “Space-air-ground integrated networks: Outage performance analysis,” *IEEE Trans. Wireless Commun.*, vol. 19, no. 12, pp. 7897–7912, 2020.
- [2] J. Liu et al., “Space-air-ground integrated network: A survey,” *IEEE Commun. Surveys Tuts.*, vol. 20, no. 4, pp. 2714–2741, 2018.

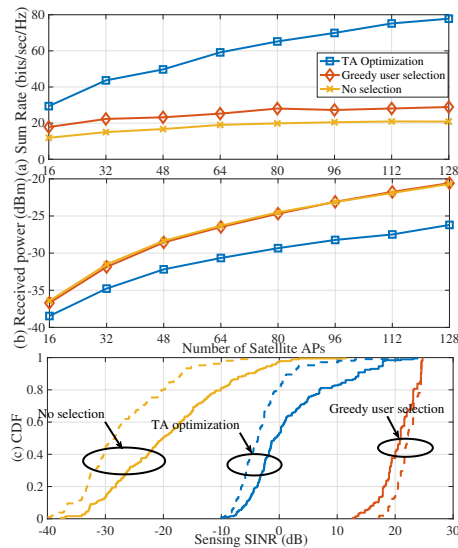


Fig. 3: (a): Sum rate performance versus number of satellite APs M . (b): Received power versus number of satellite APs. (c): CDF plot of sensing SINR under low (16-80) and high (96-128) number of APs.

- [3] V. Chien et al., "Joint power allocation and user scheduling in integrated satellite-terrestrial cell-free massive MIMO IoT systems," *IEEE Internet Things J.*, vol. 11, no. 20, pp. 32 883–32 900, Jul. 2024.
- [4] L. Yin et al., "Integrated sensing and communications enabled low earth orbit satellite systems," *IEEE Netw.*, vol. 38, no. 6, pp. 252–258, Nov. 2024.
- [5] W. D. Lukito et al., "Learning to design transceiver for integrated sensing and communications: A satellite communications perspective," *IEEE Trans. Wireless Commun.*, vol. 24, no. 9, pp. 7409–7423, Sep. 2025.
- [6] H. Yu et al., "Active channel sparsification for uplink massive MIMO with uniform planar array," *IEEE Trans. Wireless Commun.*, vol. 20, no. 9, pp. 6018–6032, 2021.
- [7] B. Mao et al., "On an intelligent hierarchical routing strategy for ultra-dense free space optical low earth orbit satellite networks," *IEEE J. Sel. Areas Commun.*, vol. 42, no. 5, pp. 1219–1230, 2024.
- [8] B. R. Bowring, "Transformation from spatial to geographical coordinates," *Surv. Rev.*, vol. 23, no. 181, pp. 323–327, 1976.
- [9] B. Hofmann-Wellenhof et al., *Global Positioning System: Theory and Practice*. Springer Sci. Bus. Media, 2012.
- [10] H. C. So, *Source Localization: Algorithms and Analysis*, 2019, ch. 3, pp. 59–106, John Wiley & Sons, Ltd, 2019.
- [11] J. He et al., "RSS localization in cell-free massive MIMO: Algorithms, analysis, and implementation," *IEEE Trans. Wireless Commun.*, vol. 25, pp. 4021–4037, 2026.
- [12] R. Radhakrishnan et al., "Survey of inter-satellite communication for small satellite systems: Physical layer to network layer view," *IEEE Commun. Surveys Tuts.*, vol. 18, no. 4, pp. 2442–2473, 2016.
- [13] M. B. Khalilsarai et al., "FDD massive MIMO via UL/DL channel covariance extrapolation and active channel sparsification," *IEEE Trans. Wireless Commun.*, vol. 18, no. 1, pp. 121–135, 2018.